

Exponentially Tilted Gaussian Prior for Variational Autoencoder

Griffin Floto¹ Stefan Kremer² Mihai Nica³

Abstract

An important property for deep neural networks to possess is the ability to perform robust out-of-distribution detection (OOD) on previously unseen data. This property is essential for safety purposes when deploying models for real world applications. Recent studies show that probabilistic generative models can perform poorly on this task, which is surprising given that they seek to estimate the likelihood of training data. To alleviate this issue, we propose the exponentially tilted Gaussian prior distribution for the Variational Autoencoder (VAE). With this prior, we are able to achieve state-of-the-art results using just the negative log-likelihood that the VAE naturally assigns, while being orders of magnitude faster than some competitive methods. We also show that our model produces high quality image samples which are more crisp than that of a standard Gaussian VAE. The new prior distribution has a very simple implementation which uses a Kullback–Leibler divergence that compares the difference between a latent vector’s length, and the radius of a sphere.

1. Introduction

For deep learning models to be safely deployed, they must be able to make reliable and accurate predictions when faced with data that is outside the training distribution. Data of this type is referred to as out-of-distribution (OOD), and highlights serious safety concerns if deep learning models cannot perform properly when receiving this type of data. For example, in the case of medical diagnosis a serious failure case would occur if a given sample is OOD and the model confidently returns a negative diagnosis. Problems of this type can be generally described as robustness to distributional shift, where a potential solution could be to detect if a shift has occurred, then decline to make a prediction

¹School of Engineering, University of Guelph, Guelph, Canada

²School of Computer Science, University of Guelph ³Department of Mathematics and Statistics, University of Guelph. Correspondence to: Griffin Floto <gfloto@uoguelph.ca>.

when an input sample is OOD. The ability to effectively handle distributional shift has been identified to be crucial to the development of effective AI systems (Amodei et al., 2016). A natural dichotomy of approaches to deal with this problem are supervised and unsupervised training. Due to the fundamental differences between the training procedures, the methods cannot easily transfer from one domain to another. The benefit of unsupervised methods is that they are more practical to use in real world applications, given that labelling data is very expensive. This type of solution will be investigated in our study.

Deep probabilistic generative models such as variational autoencoders (VAEs) (Kingma & Welling, 2014), normalizing flows (Kingma & Dhariwal, 2018) and auto-regressive models (van den Oord et al., 2016) are appealing candidates for methods that could successfully detect OOD samples in an unsupervised manner, given that they approximate the likelihood of training data. Despite this, it has been discovered that these models perform surprisingly poorly on OOD data (Nalisnick et al., 2019a) (Choi et al., 2019). To remedy this, numerous new methods have been developed, however to the best of our knowledge no general solution exists. Many of these studies propose new scores rather than using the log-likelihood which is a natural statistic of the network. Intriguingly, there appears to be an important difference between VAEs and other generative models with respect to OOD detection. A notable study (Xiao et al., 2020) found that many of the solutions to the OOD problem that were effective on generative models like normalizing flows, performed significantly worse on VAEs.

Some works have shown that more expressive prior distributions for VAEs can be used to perform well on OOD detection, without the introduction of new scores (Havtorn et al., 2021) (Maaløe et al., 2019). Following this line of work, our proposed method uses an exponentially tilted version of the standard Gaussian prior for VAEs which results in a more expressive prior. The benefit of this method for OOD detection is that no additional training data or augmentation is required, runtime is not effected, and additional scores are not introduced. We compare existing methods for OOD detection with VAEs and demonstrate that our proposed method matches or improves upon the state-of-the-art in a number of tests.

2. Method

2.1. Review of the Evidence Lower Bound Objective for the VAE

Consider a dataset $X = \{x^i\}_{i=1}^N$ that consists of N i.i.d. samples of some variable $x_i \in \mathbb{R}^{d_x}$. We assume that the data is produced by a random process which is conditioned on an unobserved variable $z \in \mathbb{R}^{d_z}$. The data generation process consists of first taking a sample from the prior distribution $p_{\theta^*}(z)$, then a value x^i is produced by the generator or decoder $p_{\theta^*}(x^i|z)$. Both the true parameters θ^* and the value of the latent variables z^i are unknown. We would like to minimize the marginal log-likelihood of the data $\sum_{i=1}^N \log p_{\theta}(x^i)$, however the integral over the latent variables is intractable. The evidence lower bound is commonly used to deal with this problem by introducing an inference model or encoder $q_{\phi}(z|x)$ to approximate the true posterior $p_{\theta}(z|x)$. Given an encoder model, the ELBO can be written as

$$\log p(x^i) \geq \mathbb{E}_{q_{\phi}(z|x^i)} [\log p_{\theta}(x^i|z)] - D_{\text{KL}}(q_{\phi}(z|x) \| p_{\theta}(z)) \quad (1)$$

where $D_{\text{KL}}(\cdot)$ is the Kullback-Leibler divergence (KLD). The KLD term in the equation above is commonly interpreted as fitting the aggregated posterior $q_{\phi}(z|x)$ to a pre-determined prior $p_{\theta}(z)$. Typically, the standard Gaussian distribution $\mathcal{N}(0, I)$ is used as the prior. By assuming an encoder distribution of $\mathcal{N}(\mu, \sigma I)$ where $\sigma = [\sigma_0 \dots \sigma_{d_z-1}]^T$, the model then has a KLD divergence of $D_{\text{KL}} = \langle \mathcal{N}(0, I) \| \mathcal{N}(\mu, \sigma I) \rangle$ which can be written as

$$D_{\text{KL}} = \frac{1}{2} \sum_{i=1}^N (\sigma_i^2 + \mu_i^2 - 1 - \log \sigma_i^2). \quad (2)$$

The lower bound of $\sum_{i=1}^N \log p_{\theta}(x^i)$ w.r.t to the parameters ϕ and θ can be optimized using the back-propagation algorithm and the “reparameterization trick” (Kingma & Welling, 2014) in which $z^i = \mu^i + \epsilon \odot \sigma^i$ where $\epsilon \sim \mathcal{N}(0, I)$.

2.2. Exponentially Tilted Gaussian Prior

The primary technical contribution of this paper is the proposal of an alternative prior distribution, namely the exponentially tilted Gaussian prior or tilted prior for short. The guiding intuition behind this work is that the standard Gaussian prior is unsuitable, as it’s minimum KLD occurs under a degenerate encoder mapping, which is commonly referred to as “posterior collapse”. In other words, the KLD term

in the log-likelihood bound forces all latent points into the same location, $\mu_i = 0$ and $\sigma_i = 1$. Under this scenario, the prior $p_{\theta}(z)$ and approximate posterior $q_{\phi}(z|x)$ are identical and the KLD is equal to 0. This condition implies that there is no available information to differentiate between encoded data samples (Hoffman & Johnson, 2016) (Alemi et al., 2018).

For $\tau \in \mathbb{R}^+$ the exponentially tilted Gaussian distribution on \mathbb{R}^{d_z} is defined by the density $\rho_{\tau} : \mathbb{R}^{d_z} \rightarrow \mathbb{R}^+$

$$\rho_{\tau}(z) = \frac{e^{+\tau\|z\|}}{Z_{\tau}} \frac{e^{-\frac{1}{2}\|z\|^2}}{\sqrt{2\pi}^{\frac{d_z}{2}}} dz \quad (3)$$

This distribution will be denoted by $e^{+\tau\|z\|} \mathcal{N}(0, I)$ to indicate that it is the standard Gaussian with an exponential tilt of τ applied to it. The additional tilting term pushes the distribution towards values of greater $\|z\|$. It is useful to note that by completing the square, the density is proportional to $e^{-\frac{1}{2}(\|z\| - \tau)^2}$, meaning that the distribution is radially symmetric and has a maximum value at τ . Figure 1 shows a plot of the distribution.

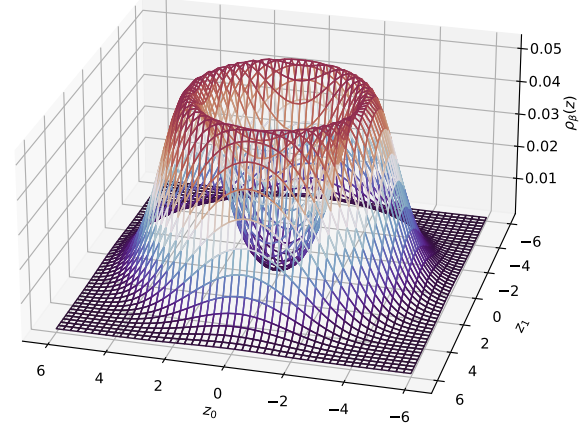


Figure 1. Probability density function of the exponentially tilted Gaussian distribution for $\tau = 3, d_z = 2$

An important feature of our method is that the encoder distribution is **not** exponentially tilted. The intention of this design is that given $\tau > 0$ there will always be a non-zero KLD between the prior and encoder distribution, meaning that $D_{\text{KL}}(q_{\phi}(z|x) \| e^{+\tau\|z\|} \mathcal{N}(0, I)) > 0$. For the sake of con-

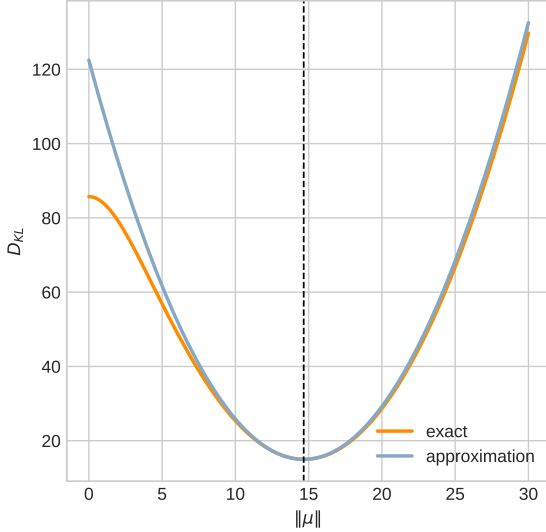


Figure 2. Comparison between the exact and quadratic approximation of the KLD for $d_z = 10, \tau = 15$

venience we now refer to $D_{\text{KL}}(q_{\phi}(z|x) \| e^{+\tau\|z\|} \mathcal{N}(0, I))$ as D_{KL}^{τ} .

Intuitively, this construction allows encoder distributions to be spread around the surface of a hyper-sphere under a minimum KLD, rather than located at the single point $\mu_i = 0$ in the case when the prior is a standard Gaussian. This work follows [31] in that we use an alternative prior that has a committed rate of δ , where $D_{\text{KL}}^{\tau} \geq \delta$. The committed rate can be interpreted as the minimum average amount of information in nats that each sample contains after being encoded. The decoder is then able to use this information to differentiate distributions in the latent space.

2.3. Normalization Constant and KL-Divergence

The calculation of the distributions normalization constant Z_{τ} and D_{KL}^{τ} is differed to Appendix A-B and summarized below. First, Z_{τ} can be written as

$$Z_{\tau} = M\left(\frac{d_z}{2}, \frac{1}{2}, \frac{1}{2}\tau^2\right) + \tau\sqrt{2} \frac{\Gamma(\frac{d_z+1}{2})}{\Gamma(\frac{d_z}{2})} M\left(\frac{d_z+1}{2}, \frac{3}{2}, \frac{1}{2}\tau^2\right) \quad (4)$$

where M stands for the Kummer confluent hypergeometric function $M(a, b, z) = \sum_{n=0}^{\infty} \frac{a^{(n)} z^n}{b^{(n)} n!}$ and $a^{(n)}$ is the rising factorial $a^{(n)} = a(a+1)\dots(a+n-1)$.

To allow for a solution that is feasible to implement computationally, it is assumed that the encoder distribution is a Gaussian with a covariance matrix $\Sigma = I$, whereas it is more commonly assumed that $\Sigma = \sigma I$. The solution to the KLD can then be written as

$$D_{\text{KL}}^{\tau}(\mu) = \log Z_{\tau} - \tau \sqrt{\frac{\pi}{2}} L_{\frac{1}{2}}^{\frac{d_z}{2}-1} \left(-\frac{\|\mu\|^2}{2} \right) + \frac{1}{2} \|\mu\|^2 \quad (5)$$

where L is the generalized Laguerre polynomial which can be defined as $L_n^{(\alpha)}(x) = \binom{n+\alpha}{n} M(-n, \alpha+1, x)$. Given the complexity of this function, it would be difficult to properly implement the back-propagation algorithm. We instead propose to use the following quadratic approximation of the KLD

$$D_{\text{KL}}^{\tau}(\mu) \geq \frac{1}{2} (\|\mu\| - \gamma)^2 + D_{\text{KL}}^{\tau}(\gamma). \quad (6)$$

where $\gamma = \text{argmin}_{\|\mu\|} D_{\text{KL}}^{\tau}(\mu)$, which can be arrived at numerically by using gradient descent. The bound is discussed in the Appendix C. Figure 2 shows an example of the difference between the exact and approximate KLD. After training the model is complete, back-propagation is no longer required meaning that the true KLD can be used to obtain a tighter bound on the log-likelihood.

2.4. Sampling from Aggregated Posterior

Typically, in order to generate samples from the model, a latent vector z will be randomly sampled from the prior, then passed through the decoder network. In our case, the aggregated posterior is slightly different from the prior distribution, thus we argue that a different sampling procedure should be employed.

Given that the KL-divergence term is invariant with respect to angular directions, we expect the aggregated posterior $q_{\phi}(z|x)$ to be approximately uniformly distributed on concentric spheres. As for the radial direction, we observe that the aggregated posterior is normally distributed whereas the prior distribution $e^{+\tau\|z\|} \mathcal{N}(0, I)$ is not. By central limit theorem type arguments, it is reasonable to expect that $q_{\phi}(z|x)$ is well approximated by a normal distribution given the prior.

Given the KLD term in the log-likelihood bound, it might be expected that the average value of $\|z\|$, which we denote $\bar{z} = \frac{1}{N} \sum_{i=1}^N \|z^i\|$ would be approximately equal to γ , however we consistently observe $\bar{z} > \gamma$. This implies that latent vectors with a larger $\|z\|$ allow the decoder to generate

data with lower reconstruction error, resulting in a better optimize the log-likelihood bound.

In Appendix D we experimentally show that $\|z\|$ when $z \sim q_\phi(z|x)$ follows the distribution $\mathcal{N}(\bar{z}, 1)$ and display a comparison between \bar{z} and γ across a variety of test parameters. As a result of these observations, we propose a two step procedure to sample from the model. First generate a vector $U \in \mathbb{R}^{d_z}$ on the unit sphere in d_z dimensions (This can be done efficiently by sampling a standard Gaussian in \mathbb{R}^{d_z} , and scaling the resulting vector to length one.) Then, scale the length by a sample from the distribution to be length $r \sim \mathcal{N}(\bar{z}, 1) \in \mathbb{R}$. The resulting sample is:

$$z_{\text{sample}} = rU \in \mathbb{R}^{d_z} \quad (7)$$

2.5. Out-of-Distribution Detection

To detect OOD samples, a one-sided threshold method is used. Scores less than or equal to the threshold are considered to be in-distribution, and scores greater than the threshold are considered to be out-of-distribution. We choose not to use the importance weighted autoencoder bound (IWAE) (Finke & Thiery, 2019) which is used by a number of current methods (Xiao et al., 2020) (Ren et al., 2019). While the IWAE can achieve a tighter bound on the log-likelihood, it is slower than using the KL-divergence and does not improve the performance of detecting OOD samples with the tilted prior. We use the l_2 reconstruction loss to calculate $\mathbb{E}_{q_\phi(z|x)} \log [p_\theta(x|z)]$. In summary, the method we use to score OOD samples is the lower bound on the log-likelihood which is written as

$$\mathcal{S}_{\text{OOD}} = \|p_\theta(x|z) - x\| + \frac{1}{2} (\|z\| - \gamma)^2 \quad (8)$$

3. Related Work

3.1. Alternative Priors for Variational Autoencoders

Arguably the most commonly used prior distribution for the VAE is the standard Gaussian, which takes the form $\mathcal{N}(0, \sigma I)$ where $\sigma = [\sigma_0 \dots \sigma_{n-1}]^\top$. While this formulations has seen great popularity, there are a number of drawbacks such as the posterior collapse problem and blurry image reconstructions due to the Gaussian distribution being uni-modal. In this section we discuss a variety of different prior distributions that have been proposed as an alternative to the standard Gaussian prior.

A popular method is to use a hierarchy of variables for the prior distribution. For example the Ladder VAE constructs a hierarchy of the form $p_\theta = p_\theta(z_L) \prod_{i=1}^{L-1} p_\theta(z_i|z_{i+1})$ where the hierarchy has L layers of latent variable. Some other example of this types of model include (Sønderby

et al., 2016), (Maaløe et al., 2016) and (Maaløe et al., 2019) which all use different ways to construct the latent variable hierarchy. The intent behind the type of method is to construct a prior which has multiple modalities and is more expressive than a standard Gaussian prior.

Another way in which a more expressive prior can be constructed is by using flow-based methods in the latent space of a VAE. This was originally proposed in (Rezende & Mohamed, 2015) with planar and radial flows as potential candidate flow methods. Many methods have been proposed that build on this idea, for example (Tomczak & Welling, 2017) which creates flows with the Householder transformation while (Kingma et al.) uses an autoregressive model.

The last type of method we review use a “committed rate” which is introduced in (Razavi et al., 2019) and refers to a lower bound on the KL-divergence of the form $D_{\text{KL}} \geq \delta$ where δ is a flexible parameter. This has the advantage of encoding more information in the latent space and prevents posterior collapse *a priori*. Razavi uses a correlated sequential model to achieve their flexible committed rate. A different line of work uses the vMF distribution $\text{vMF}(\mu, \kappa)$ with a fixed κ as a posterior and $\text{vMF}(\cdot, 0)$ as the prior. A drawback to this method is that it does not allow higher KL-divergence for different points, something which has been shown to be useful for detecting outliers in (van den Oord et al., 2017).

3.2. Unsupervised Out-of-Distribution Detection Methods

A variety of methods have been proposed to improve the performance of unsupervised methods on OoD detection. Initially, it was proposed that a one-sided log-likelihood test would be a sufficient test statistic (Choi & Chung, 2020). Since the discovery that this methodology appears to fail on many different types of generative models, many alternative scores have been proposed. Likelihood Ratios (Ren et al., 2019) proposes to use the ratio between two different types of networks, one that captures the semantic content of data, and the other which captures background information. Likelihood Regret (Xiao et al., 2020) uses a similar principle, but uses the ratio between the optimal network for the training data and the optimal network for an individual sample. ROSE (Choi et al., 2019) uses a method to compute how much a sample would update a models parameters. While each of the above stated methods lead to impressive results, one drawback is that the processes are significantly slower than the original VAE forward pass.

Input complexity (Serrà et al., 2020) shows that OOD performance can be improved by using an estimate of the Kolmogorov complexity alongside the one-sided log-likelihood test. In the case of images, the authors propose to use popular image compression algorithms like JPEG2000 as the com-

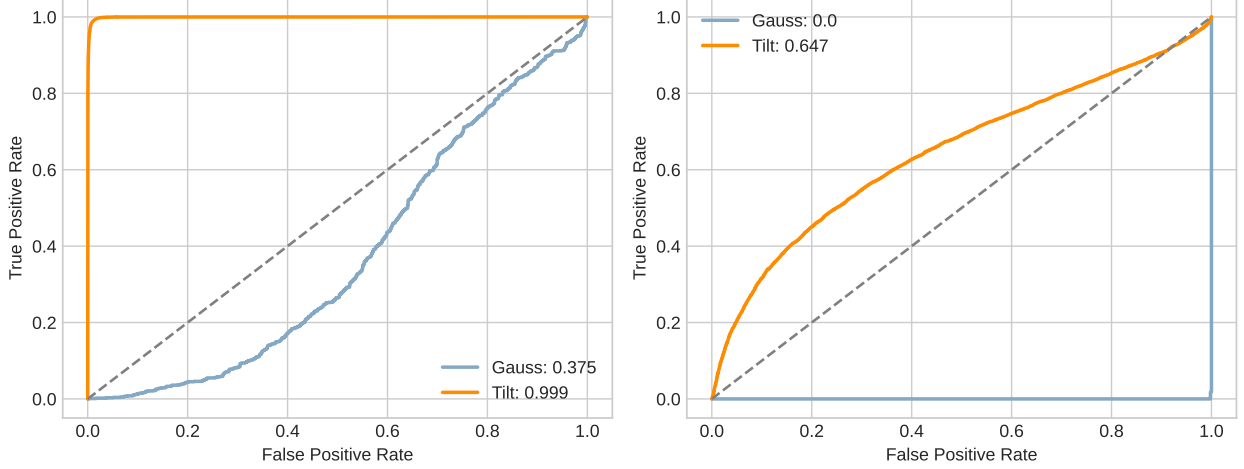


Figure 3. A comparison of the ROC of models trained with a standard Gaussian prior and an tilted prior. The left plot is data from models trained on Fashion-MNIST and the right graph is data from models trained on CIFAR-10. Both cases are tested on the MNIST dataset. The numbers in the legend are the area under the ROC.

plexity estimate, which achieves impressive performance on both normalizing flows and VAEs. Density of States Estimation (Morningstar et al., 2021) uses the idea to calculate the probability of a model probability and estimates which model statistic from a set should be used under different circumstances.

Some new scores use batch properties to generate better results. Nalisnick uses a typicality test which requires at least a pair of images per batch to function (Nalisnick et al., 2019b) and Song uses batch normalization statistics (Song et al., 2019). An immediate difficulty with using these methods in practice is that data must either be fully batched by training data or OOD in the case of [7] which is impractical, or the performance of the detection is tied to the ratio of in distribution vs OOD data in the case of [8].

A different class of methods uses OOD samples in the training process along with a procedure to encourage a network to learn to differentiate between OOD samples and the training data. Examples of this type of training include (Lee et al., 2018), which uses a GAN generator to create OOD samples and (Hendrycks et al., 2019) which uses a completely disjoint dataset to train with for example CIFAR-10 trained with CIFAR-100 as OOD. Some papers use perturbations of input images to create a data that is considered to be OOD. Choi (Choi & Chung, 2020) uses blurred images as adversarial examples, and Ran (Ran et al., 2021) adds Gaussian noise to images and employs a noise contrastive prior for the VAE architecture.

Finally (Havtorn et al., 2021) and (Maaløe et al., 2019) make use of a hierarchical latent variable prior for the VAE.

They show that the increased expressiveness of the prior improves the VAE’s ability to perform OOD detection. These works point to the possibility of performing unsupervised OOD detection using VAE’s using just the log-likelihood as a test statistic, and without any additional perturbed training data.

4. Results

In this section we conduct a basic experiment demonstrating the effect of using the tilted prior compared to the standard Gaussian prior. Details regarding the experimental settings can be found in Appendix E¹. When a VAE with a standard Gaussian prior is trained on the Fashion-MNIST and CIFAR-10 dataset, we observe that in both instances the MNIST dataset is scored with a higher log-likelihood than the training dataset. By using our proposed tilted prior, we observe that the VAEs give a much more reasonable score to the OOD MNIST dataset. The ROC are plotted for both tests in Figure 3. The tilted prior improves performance for the AUCROC metric on the Fashion-MNIST test from 0.375 to 0.999 and from 0 to 0.73 on the CIFAR-10 test. Importantly, this type of failure is not limited to these datasets, but is a pervasive issue that occurs in a large number of OOD datasets.

¹Code is available at https://github.com/gflogo/tilted_prior

Table 1. AUROC comparison between OOD detection methods with Fashion-MNIST and CIFAR-10 as training distributions. A larger number is better.

DATASET	LL	IC (PNG)	IC (JP2)	RATIO	REGRET	TILT
FASHION-MNIST						
MNIST	0.375	0.993	0.351	0.965	1.0	1.0
CIFAR-10	0.999	0.97	1.0	0.914	0.986	0.997
SVHN	0.999	0.999	1.0	0.761	0.989	0.98
KMNIST	0.765	0.863	0.769	0.96	0.998	0.999
NOISE	1.0	0.324	1.0	1.0	0.998	1.0
CONSTANT	0.975	1.0	0.984	0.98	0.777	0.797
CIFAR-10						
MNIST	0.001	0.985	0.0	0.032	0.986	0.797
FASHION-MNIST	0.032	0.991	0.036	0.335	0.976	0.688
SVHN	0.204	0.942	0.221	0.732	0.912	0.143
LSUN	0.845	0.333	0.833	0.508	0.606	0.933
CELEBA	0.693	0.310	0.679	0.404	0.738	0.877
NOISE	1.0	0.029	1.0	0.98	0.851	1.0
CONSTANT	0.016	0.999	0.282	0.98	0.905	0.0

4.1. Comparison to other Methods on Out-of-Distribution Detection

To further validate the performance of our proposed prior, we compare the tilted prior to a variety of recent methods that achieve top performance in OOD detection for VAE’s. The methods we compare against are Likelihood Regret (**Regret**) (Xiao et al., 2020), Likelihood Ratios (**Ratio**) (Ren et al., 2019), Input Complexity (**IC (png)**), (**IC (jp2)**) (Serrà et al., 2020) and a VAE with a standard Gaussian prior (**LL**). The results from this analysis are summarized on Table 1.

Overall, we observe that the tilted prior performs well in comparison to the other OOD detection methods. In 6 of the test cases we achieve top performance, compared to the next best method Input Complexity, which achieves top performance in 4 of the test cases. A failure case of our method occurs when the complexity of the OOD samples are far below that of the training data, which can be best seen in the CIFAR-10 vs Constant and the CIFAR-10 vs SVHN tests. Our best performance is achieved when the training and OOD complexity are roughly similar, as is the case for CIFAR-10 vs LSUN or CelebA and Fashion-MNIST vs KMNIST tests.

4.2. Speed Comparison

In this section we compare the runtime performance of the OOD detection models in the previous section. We use 256 IWAE samples for Likelihood Regret, Likelihood Ratio and Input Complexity which are computed in a single batch. The tilted prior computes the KL-divergence and reconstruction error in one sample, meaning that we can exploit batch processing to be at least $\mathcal{O}(b)$ faster than methods which use IWAE, where b is the batch size. To include a more

fair test, we also plot the run time for our method under the scenario where b latent vectors are sampled from the encoder which are used to obtain a more accurate estimate of $\mathbb{E}_{q_\phi(z|x)} [\log p_\theta(x|z)]$. We label this test **Tilt (batch)**.

We observe that the tilted prior has significantly faster run-time than other methods that are used to detect OOD images. In the instance where the tilted prior is exploiting batch speed-ups, we see runtime improvements of up to 4 orders of magnitude. This makes our method appealing for applications where power and timing requirements are important.

Table 2. Runtime comparison between methods on the Fashion-MNIST dataset. A larger number is better. The test is performed using a NVIDIA RTX 3090 and an AMD Ryzen 7 3800X

METHOD	IMAGES PER SECOND
TILT	4.14×10^4
TILT (BATCH)	1.61×10^2
IC (PNG)	1.02×10^2
IC (JP2)	1.00×10^2
RATIO	4.26×10^1
REGRET	2.51×10^0

4.3. Sample Quality and Log-Likelihood

Here we compare the sample quality and log-likelihood of the tilted prior to the standard Gaussian prior. We observe that the standard Gaussian prior consistently achieves a lower bound on the log-likelihood than our method. This is due to the large committed rate $D_{\text{KL}}^\tau \geq \delta = Z_\tau =$

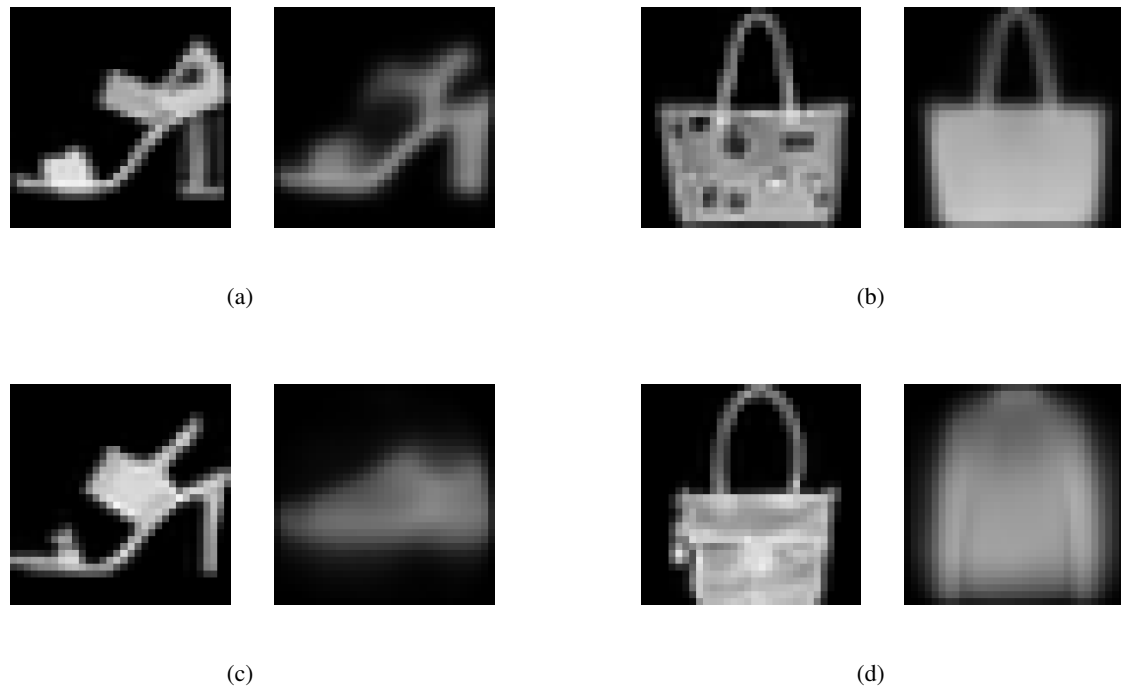


Figure 4. Comparison of reconstructed samples between the tilted prior and the standard Gaussian prior. Pairs of images correspond to the left image being from the Fashion-MNIST dataset and the right image as the reconstructed image. Images (a) and (b) are from a VAE with a tilted prior, images (c) and (d) are from a VAE with a standard Gaussian prior

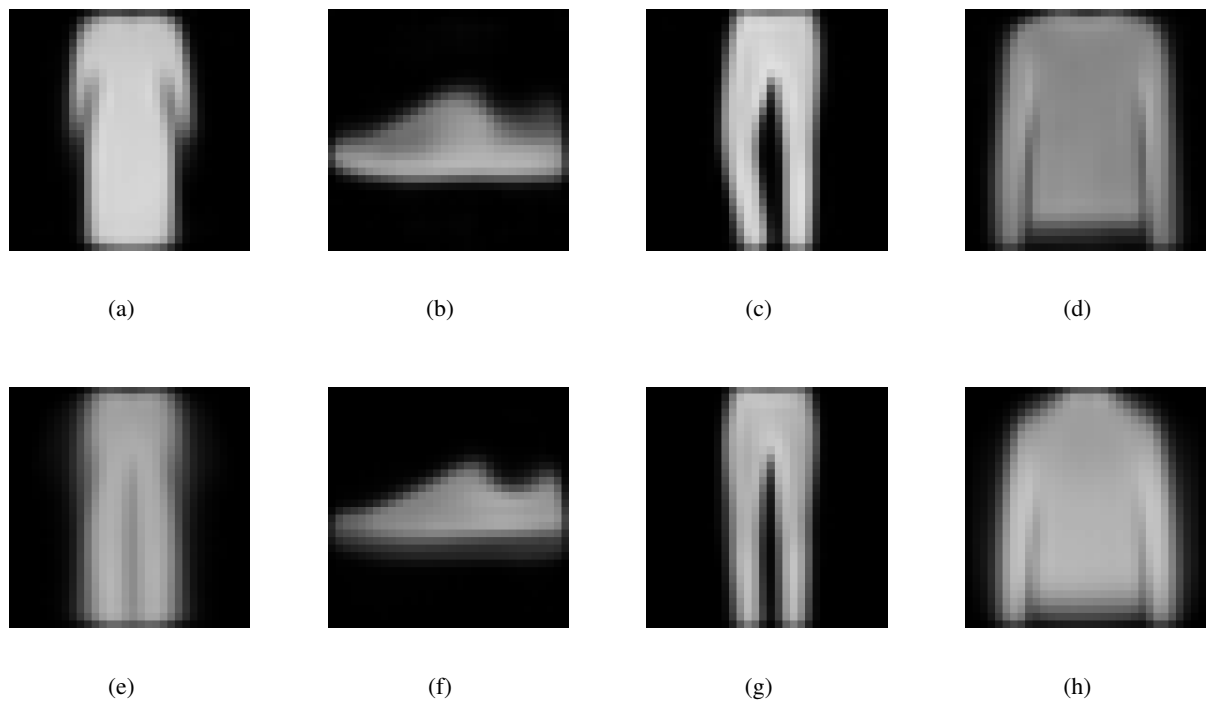


Figure 5. Comparison of image samples. Images (a)-(d) are from the tilted prior, images (e)-(f) are from the standard Gaussian prior

$M\left(\frac{d_z}{2}, \frac{1}{2}, \frac{1}{2}\tau^2\right) + \tau\sqrt{2}\frac{\Gamma(\frac{d_z+1}{2})}{\Gamma(\frac{d_z}{2})}M\left(\frac{d_z+1}{2}, \frac{3}{2}, \frac{1}{2}\tau^2\right)$ which ensures that the tilted prior must have a small τ value in order to minimize the log-likelihood bound. Given that our method lacks a learnable factorized covariance matrix $\Sigma = \sigma I$, the standard Gaussian prior is able to out-perform the tilted prior on the log-likelihood lower bound when τ is small.

Despite having low scores on the log-likelihood bound, the tilted prior still functions well as a generative model. On the task of reconstruction we observe significantly lower error than with the standard Gaussian prior. While this is also possible with an autoencoder, our method provides high quality samples from the latent space, something that is difficult for auto-encoders to do given the lack of structure in the latent space. Figures 4-5 contain examples of reconstructions and samples respectively, on a VAEs trained with the Fashion-MNIST dataset.

We observe that samples from the tilted prior appear to be more crisp than samples from the standard Gaussian prior, which are known to be “fuzzy” due to the uni-model prior. Furthermore, we observe that some data classes are completely absent from the standard Gaussian VAEs latent space which exist when using the tilted prior. Example of this can be seen in Figure 4 where the standard Gaussian VAE is unable to reconstruct the high-heel shoe type or handbag, whereas the tilted prior can.

5. Discussion

In this work we have introduced a novel prior distribution for the VAE. Through extensive testing we determined that the VAE with a tilted prior distribution can achieve state-of-the-art results on OOD detection using the natural log-likelihood test statistic. Furthermore, we show that the prior has a simple implementation and fast runtime. When sampling from the model, we find that the produced images are of high quality compared to those produced from the standard Gaussian prior. Our work supports the hypothesis that it is possible for VAEs to reliably perform unsupervised OOD detection without introducing new scores. We hope that this work can lead to further developments to improve upon the OOD detection task for VAEs.

References

Alemi, A. A., Fischer, I., and Dillon, J. V. Uncertainty in the variational information bottleneck. In *arXiv preprint arXiv:1807.00906*, 2018.

Amodei, D., Olah, C., Steinhardt, J., Christiano, P., Schulman, J., and Mané, D. Concrete problems in ai safety. In *arXiv preprint arXiv:1606.06565*, 2016.

Choi, H., Jang, E., and Alemi, A. A. Waic, but why? generative ensembles for robust anomaly detection. In *arXiv preprint arXiv:1810.01392*, 2019.

Choi, S. and Chung, S.-Y. Novelty detection via blurring. In *International Conference on Learning Representations*, 2020.

Finke, A. and Thiery, A. H. On importance-weighted autoencoders, 2019.

Havtorn, J. D. D., Frellsen, J., Hauberg, S., and Maaløe, L. Hierarchical vaes know what they don’t know. In *Proceedings of the 38th International Conference on Machine Learning*, pp. 4117–4128, 2021.

Hendrycks, D., Mazeika, M., and Dietterich, T. Deep anomaly detection with outlier exposure. In *International Conference on Learning Representations*, 2019.

Hoffman, M. and Johnson, M. Elbo surgery: yet another way to carve up the variational evidence lower bound. In *Advances in Approximate Bayesian Inference, NIPS Workshop*, 2016.

Kingma, D. P. and Dhariwal, P. Glow: Generative flow with invertible 1x1 convolutions. In *Advances in Neural Information Processing Systems*, 2018.

Kingma, D. P. and Welling, M. Auto-encoding variational bayes. In *arXiv preprint arXiv:1312.6114*, 2014.

Kingma, D. P., Salimans, T., Jozefowicz, R., Chen, X., Sutskever, I., and Welling, M. Improved variational inference with inverse autoregressive flow. In *Advances in Neural Information Processing Systems*.

Lee, K., Lee, H., Lee, K., and Shin, J. Training confidence-calibrated classifiers for detecting out-of-distribution samples. In *International Conference on Learning Representations*, 2018.

Maaløe, L., Sønderby, C. K., Sønderby, S. K., and Winther, O. Auxiliary deep generative models. In *Proceedings of The 33rd International Conference on Machine Learning*, pp. 1445–1453, 2016.

Maaløe, L., Fraccaro, M., Liévin, V., and Winther, O. Biva: A very deep hierarchy of latent variables for generative modeling. In Wallach, H., Larochelle, H., Beygelzimer, A., d’Alché-Buc, F., Fox, E., and Garnett, R. (eds.), *Advances in Neural Information Processing Systems*, 2019.

Morningstar, W., Ham, C., Gallagher, A., Lakshminarayanan, B., Alemi, A., and Dillon, J. Density of states estimation for out of distribution detection. In *Proceedings of The 24th International Conference on Artificial Intelligence and Statistics*, Proceedings of Machine Learning Research, pp. 3232–3240, 2021.

Nalisnick, E., Matsukawa, A., Teh, Y. W., Gorur, D., and Lakshminarayanan”, B. Do deep generative models know what they don’t know? In *International Conference on Learning Representations*, 2019a.

Nalisnick, E., Matsukawa, A., Teh, Y. W., and Lakshminarayanan”, B. Detecting out-of-distribution inputs to deep generative models using typicality. In *arXiv preprint arXiv:1906.02994*, 2019b.

Ran, X., Xu, M., Mei, L., Xu, Q., and Liu, Q. Detecting out-of-distribution samples via variational auto-encoder with reliable uncertainty estimation. In *arXiv preprint arXiv:2007.08128*, 2021.

Razavi, A., van den Oord, A., Poole, B., and Vinyals, O. Preventing posterior collapse with delta-vaes. In *International Conference on Learning Representations*, 2019.

Ren, J., Liu, P. J., Fertig, E., Snoek, J., Poplin, R., Depristo, M., Dillon, J., and Lakshminarayanan, B. Likelihood ratios for out-of-distribution detection. In *Advances in Neural Information Processing Systems*, 2019.

Rezende, D. and Mohamed, S. Variational inference with normalizing flows. In *Proceedings of the 32nd International Conference on Machine Learning*, pp. 1530–1538, 2015.

Serrà, J., Álvarez, D., Gómez, V., Slizovskaia, O., Núñez, J. F., and Luque, J. Input complexity and out-of-distribution detection with likelihood-based generative models. In *International Conference on Learning Representations*, 2020.

Song, J., Song, Y., and Ermon, S. nsupervised out-of-distribution detection with batch normalization. In *arXiv preprint arXiv:1910.09115*, 2019.

Sønderby, C. K., Raiko, T., Maaløe, L., Sønderby, S. r. K., and Winther, O. Ladder variational autoencoders. In Lee, D., Sugiyama, M., Luxburg, U., Guyon, I., and Garnett, R. (eds.), *Advances in Neural Information Processing Systems*, 2016.

Tomczak, J. M. and Welling, M. Improving variational auto-encoders using householder flow. In *arXiv preprint arXiv:1611.09630*, 2017.

van den Oord, A., Kalchbrenner, N., Espeholt, L., kavukcuoglu, k., Vinyals, O., and Graves, A. Conditional image generation with pixelcnn decoders. In *Advances in Neural Information Processing Systems*, 2016.

van den Oord, A., Vinyals, O., and kavukcuoglu, k. Neural discrete representation learning. In *Advances in Neural Information Processing Systems*, 2017.

Xiao, Z., Yan, Q., and Amit, Y. Likelihood regret: An out-of-distribution detection score for variational auto-encoder. In *Advances in Neural Information Processing Systems*, pp. 20685–20696, 2020.

A. Derivation of the Normalization Constant for the Tilted Gaussian

$$\rho_\tau(z) = \frac{e^{+\tau\|z\|}}{Z_\tau} \frac{e^{-\frac{1}{2}\|z\|^2}}{\sqrt{2\pi}^{d/2}} dz$$

$$\begin{aligned} Z_\tau &= \mathbb{E}_{z \sim \mathcal{N}(0, I)} [e^{\tau\|z\|}] = \int_{\mathbb{R}^d} e^{+\tau\|z\|} \frac{e^{-\frac{1}{2}\|z\|^2}}{\sqrt{2\pi}^{d/2}} dz \\ &= \mathbb{E}_{x \sim \chi(d)} [e^{\tau x}] = \int_0^\infty e^{\tau x} \frac{x^{d-1} e^{-\frac{1}{2}x^2}}{2^{\frac{1}{2}d-1} \Gamma(\frac{d}{2})} dx, \end{aligned}$$

$$\text{where } \chi \stackrel{d}{=} \|z\|$$

$$\begin{aligned} &= \sum_{n=0}^{\infty} \frac{\tau^n \mathbb{E}[\chi^n]}{n!} \\ &= \sum_{n \text{ even}}^{\infty} \frac{\tau^n d(d+2)\dots(d+n-2)}{n!} \\ &\quad + \sum_{n \text{ odd}}^{\infty} \frac{\tau^n \mu_1 (d+1)(d+3)\dots(d+n-2)}{n!} \end{aligned}$$

$$\text{where } \mu_1 = \mathbb{E}[\chi] = \sqrt{2} \frac{\Gamma(\frac{d+1}{2})}{\Gamma(\frac{d}{2})}$$

$$\begin{aligned} &= M\left(\frac{d}{2}, \frac{1}{2}, \frac{1}{2}\tau^2\right) \\ &\quad + \tau\sqrt{2} \frac{\Gamma(\frac{d+1}{2})}{\Gamma(\frac{d}{2})} M\left(\frac{d+1}{2}, \frac{3}{2}, \frac{1}{2}\tau^2\right) \end{aligned}$$

where $M(a, b, z) = \sum_{n=0}^{\infty} \frac{a^{(n)}}{b^{(n)}} \frac{z^n}{n!}$ is the Kummer confluent hypergeometric function and $a^{(n)} = a(a+1)\dots(a+n-1)$ is the rising factorial.

B. Derivation of the KL-Divergence

$$\begin{aligned} D_{\text{KL}}^\tau &= D_{\text{KL}}\left(\mathcal{N}(\mu(x), I), e^{\tau\|z\|} \mathcal{N}(0, Id)\right) \\ &= \mathbb{E}_{z \sim \mathcal{N}(\mu(x), I)} \left[\ln \left(\frac{\rho_{\mathcal{N}(\mu(x), Id)}(z)}{\rho_{e^{\tau\|z\|} \mathcal{N}(0, I)}(z)} \right) \right] \\ &= \mathbb{E}_{z \sim \mathcal{N}(\mu(x), I)} \left[\ln \left(\frac{e^{-\frac{1}{2}\|z\|^2 - \mu^2}}{\frac{1}{Z_\tau} e^{\tau\|z\|} e^{-\frac{1}{2}\|z\|^2}} \right) \right] \\ &= \mathbb{E}_{z \sim \mathcal{N}(\mu(x), I)} \left[\ln \left(Z_\tau e^{-\tau\|z\|} e^{-\frac{1}{2}\|z\|^2 + \langle z, \mu \rangle - \frac{1}{2}\|\mu\|^2 + \frac{1}{2}\|z\|^2} \right) \right] \end{aligned}$$

$$\begin{aligned} &= \ln(Z_\tau) - \tau \mathbb{E}_{z \sim \mathcal{N}(\mu(x), I)} [\|z\|] - \frac{1}{2}\|\mu\|^2 \\ &= \ln(Z_\tau) - \tau L_{\frac{1}{2}}^{(d/2-1)}\left(-\frac{\|\mu\|^2}{2}\right) - \frac{1}{2}\|\mu\|^2, \end{aligned}$$

where $\mathbb{E}_{z \sim \mathcal{N}(\mu(x), I)} [\|z\|] = \mathbb{E}[\chi_\mu] = L_{\frac{1}{2}}^{(d/2-1)}\left(-\frac{\|\mu\|^2}{2}\right)$ and $L_n^{(\alpha)}$ is the generalized Laguerre polynomial.

C. KL-Divergence Approximation Procedure

We show empirically show that

$$\begin{aligned} D_{\text{KL}}^\tau &= D_{\text{KL}}\left(\mathcal{N}(\mu(x), I), e^{\tau\|z\|} \mathcal{N}(0, I)\right) \\ &\geq \frac{1}{2} (\|\mu\| - \gamma)^2 + D_{\text{KL}}^\tau(\gamma) \end{aligned}$$

where $\gamma = \text{argmin}_{\|\mu\|} D_{\text{KL}}^\tau(\mu)$, which is found by using algorithm 1. The KLD is convex and thus the optimization procedure easily reaches the function minimum. To confirm the bound, use the following parameter search space: $d_z = [2, 3, \dots, 200]$, $\tau = 1.2^w$ where $w = [-20, -19, \dots, 25]$. A total of 10^4 evenly spaced $\|\mu\|$ points between 0 and 200 were checked for each hyper-parameter setting and we found that across the full search space the KLD bound existed.

Algorithm 1 KL-Divergence Minimization

Input: tilt τ , latent dim. d_z , learning rate lr
 Initialize $x = \sqrt{\tau^2 - d_z}$
for $i = 1$ **to** $m - 1$ **do**
 $y_1 = D_{\text{KL}}^\tau(x - dx, \tau, d_z)$
 $y_2 = D_{\text{KL}}^\tau(x + dx, \tau, d_z)$
 $\text{grad} = (y_2 - y_1)/2$
 $x = x - lr * \text{grad}$
end for
return x

D. Aggregate Posterior

In this section we show that the aggregated posterior has a radial component which is distribution according to $\mathcal{N}(\bar{z}, 1)$ and provide information about typical value of \bar{z} . Figure 4 shows the cumulative distribution function of both $q_\phi(z|x)$ and $\mathcal{N}(\bar{z}, 1)$ which are approximately identical. Table 3 shows examples of γ , \bar{z} , and σ from models trained from the Fashion-MNIST and CIFAR-10 dataset.

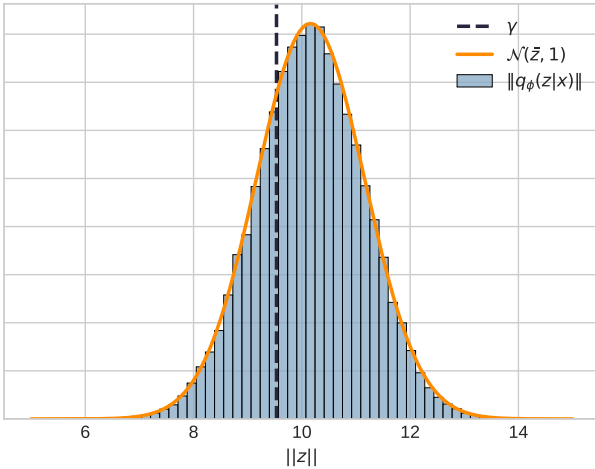


Figure 6. A comparison between the cumulative distribution function of $\mathcal{N}(\bar{z}, 1)$ and the radial component of $q_\phi(z|x)$. This test was performed on the FMINST dataset with $d_z = 10$ and $\tau = 10$.

Table 3. Example values of \bar{z} , γ and σ on the Fashion-MNIST and CIFAR-10 datasets

DATA SET	\bar{z}	σ	γ	τ	d_z
FASHION-MNIST	10.15	0.99	9.53	10	10
	19.91	1.01	19.77	20	10
	29.99	1.02	29.85	30	10
CIFAR-10	15.05	1.01	11.20	15	100
	24.92	0.97	22.93	25	100
	39.80	1.04	38.72	40	100

E. Experimental Settings

E.1. Datasets

Datasets that are used in our experiments are MNIST, Fashion-MNIST, KMNIST, CIFAR-10, SVHN, CelebA and LSUN. Following the work of (Xiao et al., 2020), we also use two synthetic datasets which we call Noise and Constant. Images from the Noise dataset are created by sampling from the uniform distribution in the range of [0, 255] for each pixel in an image, where the constant dataset is created by sampling from the uniform distribution in the range of [0, 255], where all pixels are the same value. All images are resized to shape 32 x 32. Color images are converted to grayscale for the Fashion-MNIST test by taking the first channel and discarding the other two. Grayscale images are converted to color images by taking 3 copies of the first channel. When testing with the CelebA and LSUN datasets, we use 50000 random samples from each due to the large dataset sizes.

E.2. Model Structure and Optimization Procedure

For all tests we train the VAE for 250 epochs with a batch size of 64. We use the ADAM optimizer with a learning rate of 10^{-4} and clip gradients that are greater than 100. The encoder of the VAE consists of 5 convolutional layers with a fully connected layer for both μ and σ . The decoder uses 6 deconvolutional layers and ends with a single convolutional layer. We initialize all convolutional weights from the distribution $\mathcal{N}(0, 0.2)$. On the FMNIST test we use latent dimensions $d_z = 10$ and for the CIFAR-10 test we used $d_z = 100$. Both Likelihood Regret and Likelihood Ratio are intended to be run with the cross entropy loss, thus we employ this as the reconstruction loss function for all networks except the tilted prior, which uses l_2 loss. We emphasize the importance of the fully connected layer in the encoder. This is essential as the KL-Divergence is a function of $\|\mu\|$ which is difficult to optimize with a fully convolutional model. The code for the full model can be found at: https://github.com/gfloto/tilted_prior/model.

E.3. Implementing Methods

For all comparison methods we use IWAE with 256 samples to derive a lower bound on the log-likelihood. For Likelihood Regret we use run gradient descent on all model parameters for 100 steps in each of the tests. We use the ADAM optimizer for this process at a learning rate of 1e-4, which is the same as the training procedure. We train the background model in Likelihood Ratio by setting the perturbation ratio parameter μ to be 0.2 for all tests. Besides this, the background model is trained in an identical format to the regular neural networks. For input complexity we use the OpenCV implementations of the PNG and JP2 compression algorithms. The tilted prior uses $\tau = 30$ for the Fashion-MNIST test and $\tau = 25$ for the CIFAR-10 test.